Journal of Photochemistry and Photobiology A: Chemistry 215 (2010) 164–171

Contents lists available at ScienceDirect

Journal of Photochemistry and Photobiology A: Chemistry

journal homepage: www.elsevier.com/locate/jphotochem

Laser ablation of Ga in dielectric breakdown of gaseous hydrocarbons: deposition of ambient-pressure unstable Ga nanophases in carbonaceous environment

Dana Pokorná[a], Markéta Urbanová[a], Snejana Bakardjieva[b], Jan Šubrt[b], Josef Pola[a,*]

[a] Laboratory of Laser Chemistry, Institute of Chemical Process Fundamentals, ASCR, 16502 Prague, Czech Republic
[b] Institute of Inorganic Chemistry, ASCR, 25068 Řež, Czech Republic

ARTICLE INFO

Article history:
Received 12 July 2010
Received in revised form 3 August 2010
Accepted 5 August 2010
Available online 13 August 2010

Keywords:
IR laser
Ga ablation
dielectric breakdown
hydrocarbon decomposition
gas-phase deposition
a-C:H film
ambient-pressure unstable Ga nanoforms

ABSTRACT

IR laser-irradiation of Ga in gaseous hydrocarbon (benzene, ethyne or n-hexane) results in ablation of Ga and adjacent dielectric breakdown (DB) in gaseous hydrocarbons. These processes lead to chemical vapor deposition of Ga nanoparticles-containing carbonaceous films. Volatile products of DB were examined by FTIR spectroscopy and GC and GC/MS techniques and revealed as arising from carbonization reactions in the gas phase. The solid products were analyzed by FTIR, X-ray photoelectron and Raman spectroscopy and electron microscopy and disclosed as Ga nanophases enveloped by graphite-like shell of carbonaceous phase. These nanophases include ambient pressure stable orthorhombic and amorphous structures and tetragonal, cubic and rhombohedral structures that have been previously observed only at high pressures. The reported procedure of chemical vapor deposition of the high-pressure Ga nanostructures thus represents a novel approach to these phases.

1. Introduction

There is a continuing interest in elemental gallium due to its potential applications as nano liquid-metal coolant [1], carbon nanothermometer [2], gallium-metal nanocomposites and nanostructured films for plasmonic applications [3,4], molten solvent for bulk synthesis of silicon nanowires [5] and multiwall carbon nanotubes [6], large droplets for catalytic growth of silica nanowire bunches [7] and nanoparticles for surface-enhanced Raman spectroscopy [8].

The fabrication of separated Ga nanoforms is rather difficult owing to the low melting point of Ga (29.8 °C) which makes coalescence to larger aggregates an easy process. Up to now, nanoparticles of liquid Ga have been grown by molecular beam epitaxy on sapphire [8,9] and GaN [10] substrates, liquid Ga nano-columns were prepared by heating GaN in a flow of ethyne [6] or by high-temperature reaction between Ga and methane [11], nanolayers of Ga were formed through nanoscale grain boundary penetration of Ga drop on Al film [3,4] and ordered nanostructures and nanoislands were fabricated by deposition of collimated atomic beam [12].

We have recently explored IR laser-induced metal (Co, Ni, Ag) ablation in dielectric breakdown of gaseous hydrocarbons [13–15]. The short IR laser pulses allow hydrocarbon carbonization in the plume of ablated metal particles within a temperature jump and subsequent stabilization of hot nanosized metal species by a fast (post-pulse) decrease in temperature and excess of simultaneously produced and deposited nanostructured carbon phase. The technique is suitable for fabrication of nanosized metal particles isolated in carbonaceous phase and shows a potential for synthesis of metastable nanostructures [15]. In a conjunction with our previous studies we now report on IR laser ablation of gallium in dielectric breakdown of several hydrocarbons and reveal that this process allows gas-phase deposition of nanostructured carbonaceous films containing Ga orthorhombic structures stable at ambient pressure and Ga tetragonal, cubic and rhombohedral structures that have been previously observed only at high pressures.

2. Experimental

IR-laser irradiation experiments were conducted in a Pyrex reactor (70 mL in volume) in the presence of 1 and 10 Torr of ethyne, benzene or n-hexane. The hydrocarbons were irradiated by a pulsed TEA CO_2 laser (model 1300 M, Plovdiv University) operating with a frequency of 1 Hz on the P(20) line of the $00^01\text{-}10^00$ transition (944.19 cm^{-1}) and a pulse energy of 1.8 J. This radiation was focused with a NaCl lens (focal length 15 cm) on the Ga target positioned

* Corresponding author.
E-mail address: pola@icpf.cas.cz (J. Pola).

1010-6030/$ – see front matter © 2010 Elsevier B.V. All rights reserved.
doi:10.1016/j.jphotochem.2010.08.009

in the centre of the reactor above which were accommodated copper substrates. The pulsed irradiation of Ga in the hydrocarbons took place at the reactor temperature below 20 ° C and resulted in Ga ablation and decomposition of the hydrocarbon, both of which allowed deposition of Ga/C films on the Cu substrate and on the irradiated Ga target.

The reactor was described elsewhere [15]) and it was a tube fitted at each end with KBr windows and having a port with rubber septum enabling GC and GC/MS analyses of gaseous content and a PTFE valve connecting to vacuum manifold and pressure transducer.

The progress of the hydrocarbons decomposition and volatile decomposition products were analyzed directly in the reactor by FTIR spectrometry (an FTIR Nicolet Impact spectrometer, resolution 4 cm^{-1}) using diagnostic absorption bands at 1037 cm^{-1} (benzene), 3268 cm^{-1} (ethyne) and 1465 cm^{-1} (n-hexane). Aliquots of the irradiated reactor content were sampled by a gas-tight syringe and analyzed by gas chromatography-mass spectroscopy (a Shimadzu QP 5050 mass spectrometer, 50-m Porabond capillary column, programmed temperature 30–200 °C). The decomposition products were identified through their FTIR spectral diagnostic bands (C_2H_2, 731 cm^{-1}; C_4H_2, 628 cm^{-1}; CH_4, 1305 and 3016 cm^{-1}) and through their mass spectra using the NIST library.

The deposited films were analyzed with the FTIR Nicolet Impact spectrometer, a Nicolet Almega XR Raman spectrometer (resolution 2 cm^{-1}, excitation wavelength 473 nm and power 10 mW) and by electron microscopy (a Philips XL30 CP scanning electron microscope equipped with an energy-dispersive analyzer EDAX DX-4 of X-ray radiation) and a JEOL JEM 3010 microscope operating at 300 kV and equipped with an EDS detector (INCA/Oxford) and CCD Gatan (Digital Micrograph software). The Raman spectral analysis was carried out on different microregions of the films to verify the absence of non-homogeneous spots of the films on Cu substrate and to detect differences in the spectra for the film areas near the target crater. The transmission electron analysis was carried out on ground samples that were subsequently dispersed in ethanol followed by application of a drop of a diluted suspension on a Ni grid. Diffraction patterns were measured with a PANalytical X'Pert PRO diffractometer equipped with a conventional X-ray tube (Co Ka radiation, 40 kV, 30 mA, point focus), an X-ray monocapillary with diameter of 0.1 mm, and a multichannel detector X'Celerator with an anti-scatter shield.

Benzene (Lachema, purity better than 99.7 per cent), ethyne (Linde, purity better than 98,5 per cent) and n-hexane (Lach-Ner, purity better than 99 per cent) were evaporated from the liquid nitrogen-solidified compounds on a vacuum line prior to use.

3. Results and Discussion

The TEA CO_2 laser irradiation of Ga target in the presence of gaseous hydrocarbons (1 and 10 Torr of benzene, ethyne or n-hexane) results in a visible luminescence (plume), decomposition of the hydrocarbons and deposition of Ga/C films on the Cu substrate (and the nearby reactor surface) and on the irradiated target.

The films deposited by repetitive laser pulses on the Cu substrate are noticeably thicker than those deposited on the Ga target, because a substantial fraction of the film deposited in the region of the laser plume is repeatedly removed by next pulses.

Volatile products of the decomposition of benzene are ethyne (~ 60 mole %), ethene (~ 20-24 mole %), butadiyne (~ 10 mole %) and propane, 1-buten-3-yne, C_3H_4, and ethynylbenzene (each 0.1-0.5 mole %). The products of the decomposition of ethyne are butadiyne (90-96 mole %) and C_3H_4 and 1,3-butadiene (each 2-4 mole %). The products of the decomposition of n-hexane are ethyne (64 mole %), ethene (15 mole %), methane and butadiyne (each 5-6%), ethane and propene, each 2-3 mole %) and propane, propadiene, propyne, butane and 1,3-butadiene (each 0.2-1.2 mole %). These compounds were also formed in the pyrolysis of benzene [16], ethyne [17,18] and n-hexane [19,20] and are in line with carbonization of the hydrocarbons.

The solid films deposited on Cu substrate from benzene and ethyne with 40 pulses (1 Torr) and 100 pulses (10 Torr) were black, whereas those deposited at the same conditions from n-hexane were very thin and slightly darker than the original colour of the Cu substrate. The SEM-EDX analysis of the films deposited from

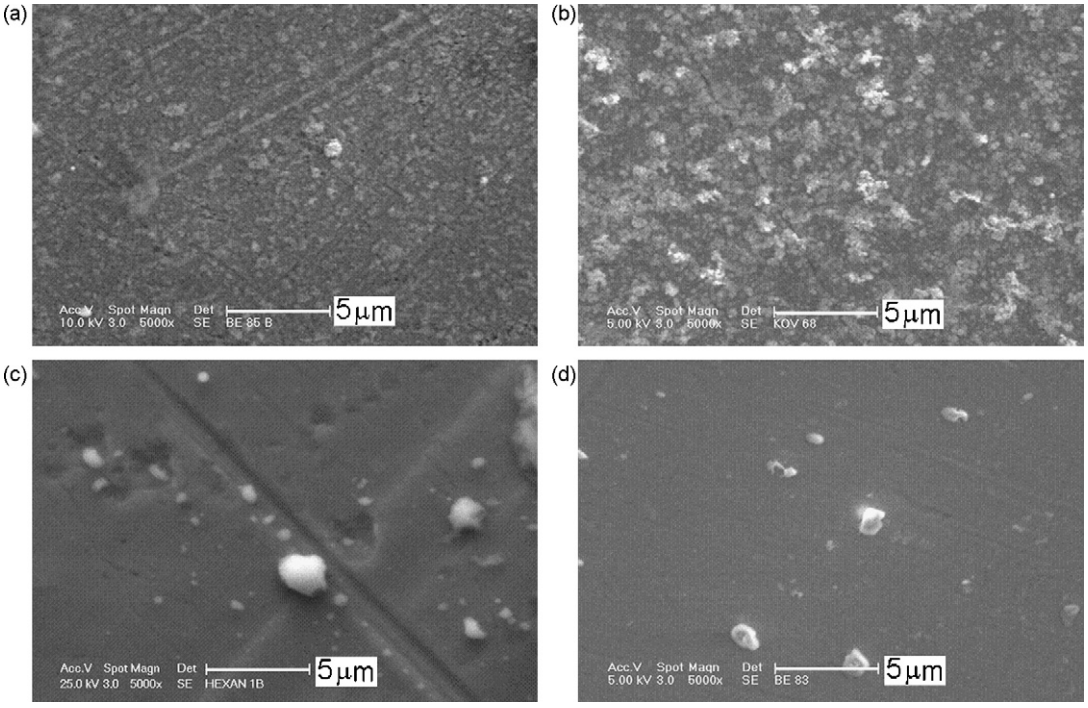

Fig. 1. SEM images of films deposited on Cu substrate from 10 Torr of benzene (a), ethyne (b), n-hexane (c) and 1 Torr of benzene (d).

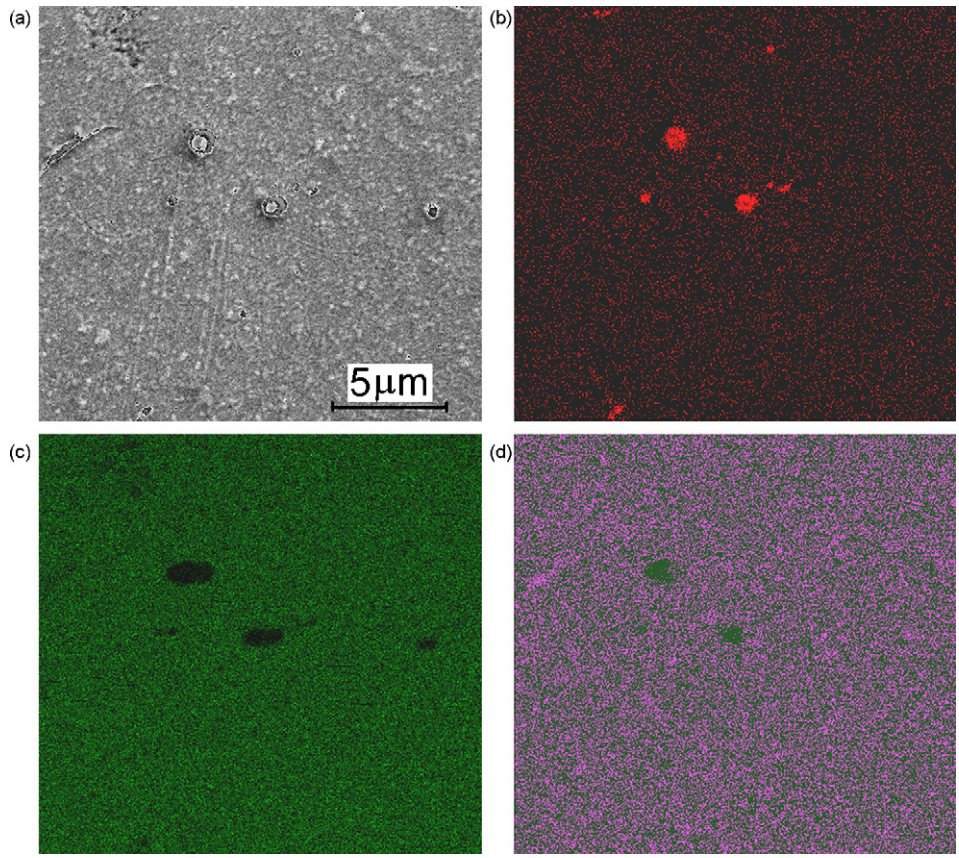

Fig. 2. SEM image of the film deposited on Cu substrate from 10 Torr of benzene (a) and SEM-EDX elemental mapping showing the corresponding Ga (L) (b, red), Cu (L) (c, green) and C (K) (d, violet) maps.

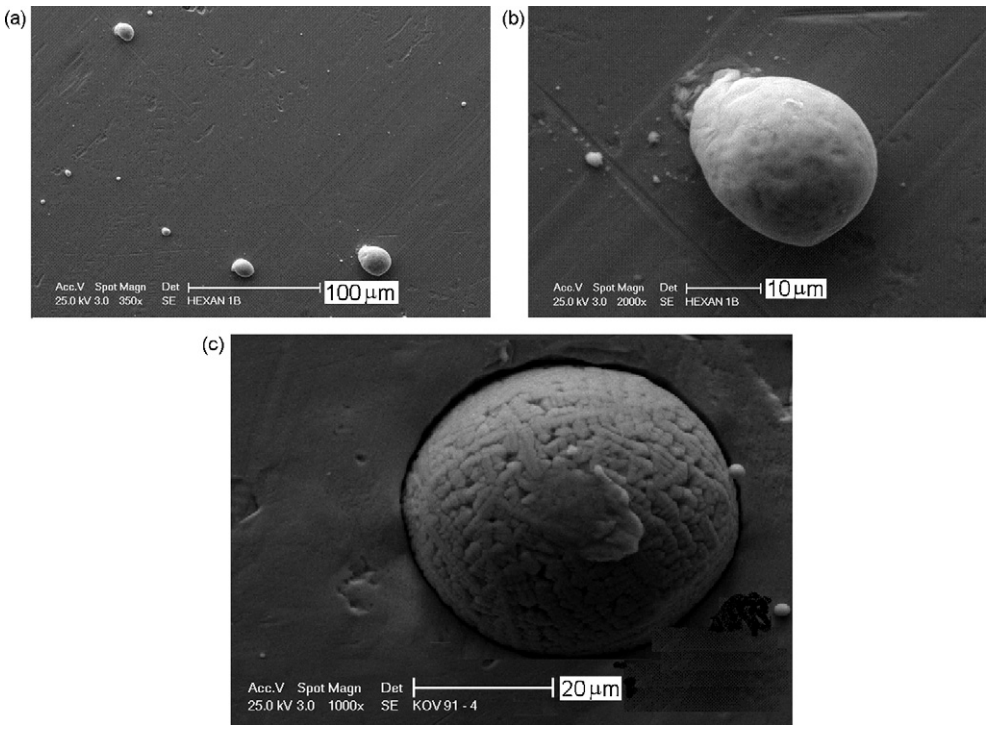

Fig. 3. SEM images of films deposited from hexane showing different sized Ga particles (a) and smooth (b) and structured (c) surface of these particles.

Table 1
Atomic per cent of Ga in carbonaceous deposit on Cu substrate..

Hydrocarbon	Pressure, Torr	Decomposition progress, %	At.% of Ga in Ga/C film
benzene	1[a]	80	8.3
	10[b]	35	4.9
ethyne	1[b]	80	12.1
	10[b]	50	2.6
n-hexane	10[b]	50	36

[a] 40 pulses.
[b] 100 pulses.

benzene and ethyne at 1 and 10 Torr shows the prevalence of carbon, traces of oxygen (less than 2-5 atomic percent of carbon) and low amounts of Ga. On the other hand, the thin films from n-hexane have high amounts of Ga and less carbon (Table 1).

The SEM images of the films deposited from 10 Torr of benzene (Fig. 1a) and ethyne (Fig. 1b) show a fluffy morphology, whereas those for the films deposited from 1 and 10 Torr of n-hexane (Fig. 1c) and from 1 Torr of ethyne and benzene (Fig. 1d) reveal distinct and less than one up to several μm-sized bodies.

SEM-EDX and elemental mapping analyses (Fig. 2) indicate that C and Ga elements are uniformly distributed over the fluffy areas and that the distinct bodies are rich for or contain solely Ga.

We note that in addition to these typical morphologies extra large smooth and structured Ga particles (ca. 10-20 μm) were also observed only for ablation in hexane (Fig. 3) and we assume that their formation is due to easier coalescence of smaller Ga bodies at low extent of hexane carbonization.

More information on the nature of the deposited films is obtained from visible Raman spectra which differ depending on which hydrocarbon has been used for the deposition process and whether the films were deposited on Cu substrate or Ga target (Figs. 4–6).

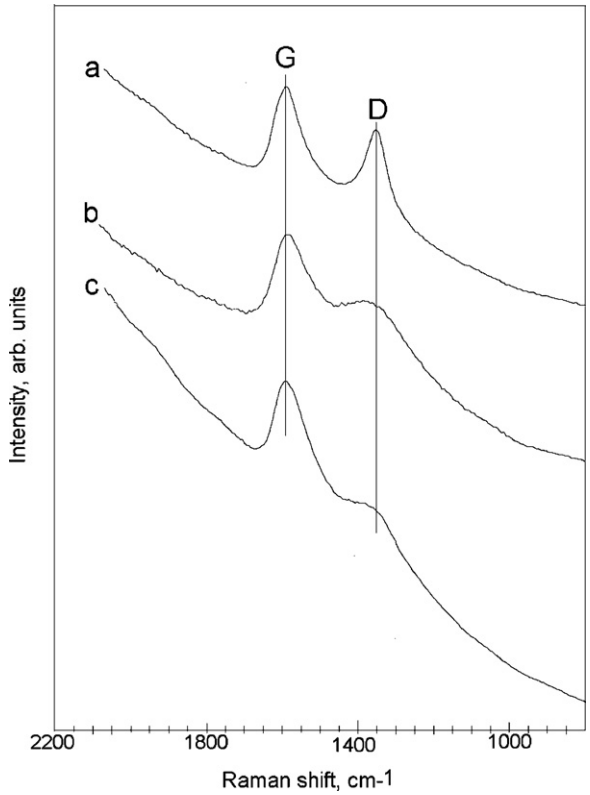

Fig. 4. Raman spectrum of film deposited from 1 Torr of benzene on Ga target (a) and from 1 Torr (b) and 10 (c) Torr of benzene on Cu substrate.

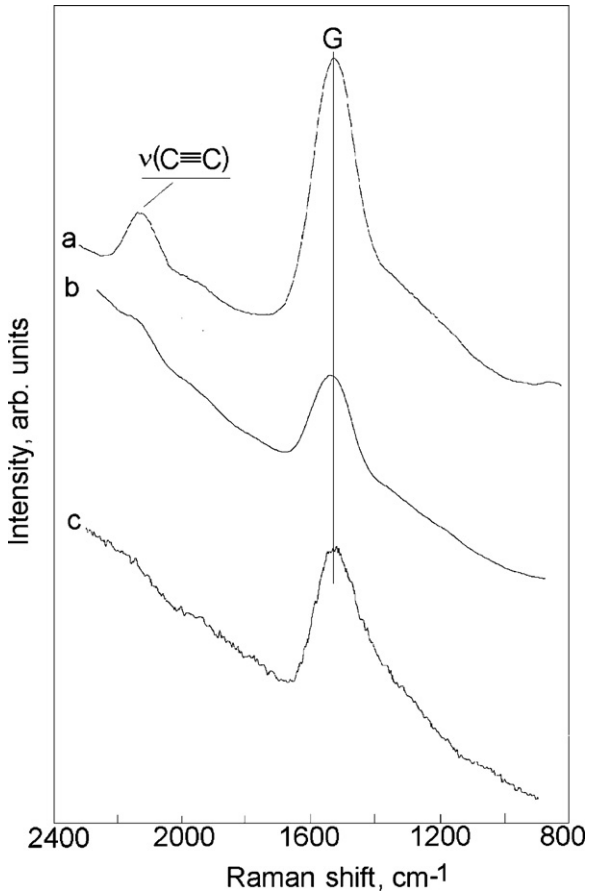

Fig. 5. Raman spectrum of film deposited from 1 Torr of ethyne on Ga target (a) and from 1 Torr (b) and 10 (c) Torr of ethyne on Cu substrate.

The spectra of black films deposited from benzene (Fig. 4) are composed of well separated G and D bands of unsaturated sp^2 carbon, which are respectively centered at 1580-1590 cm^{-1} and 1350-1360 cm^{-1}. These bands are of similar intensity for the films deposited on Ga target and have lower D/G values when deposited on Cu substrate.

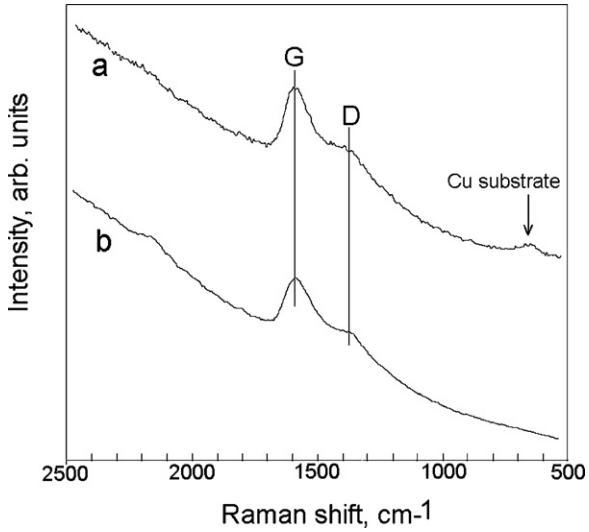

Fig. 6. Raman spectrum of film deposited on Cu substrate (a) and Ga target (b) from 10 Torr of n-hexane.

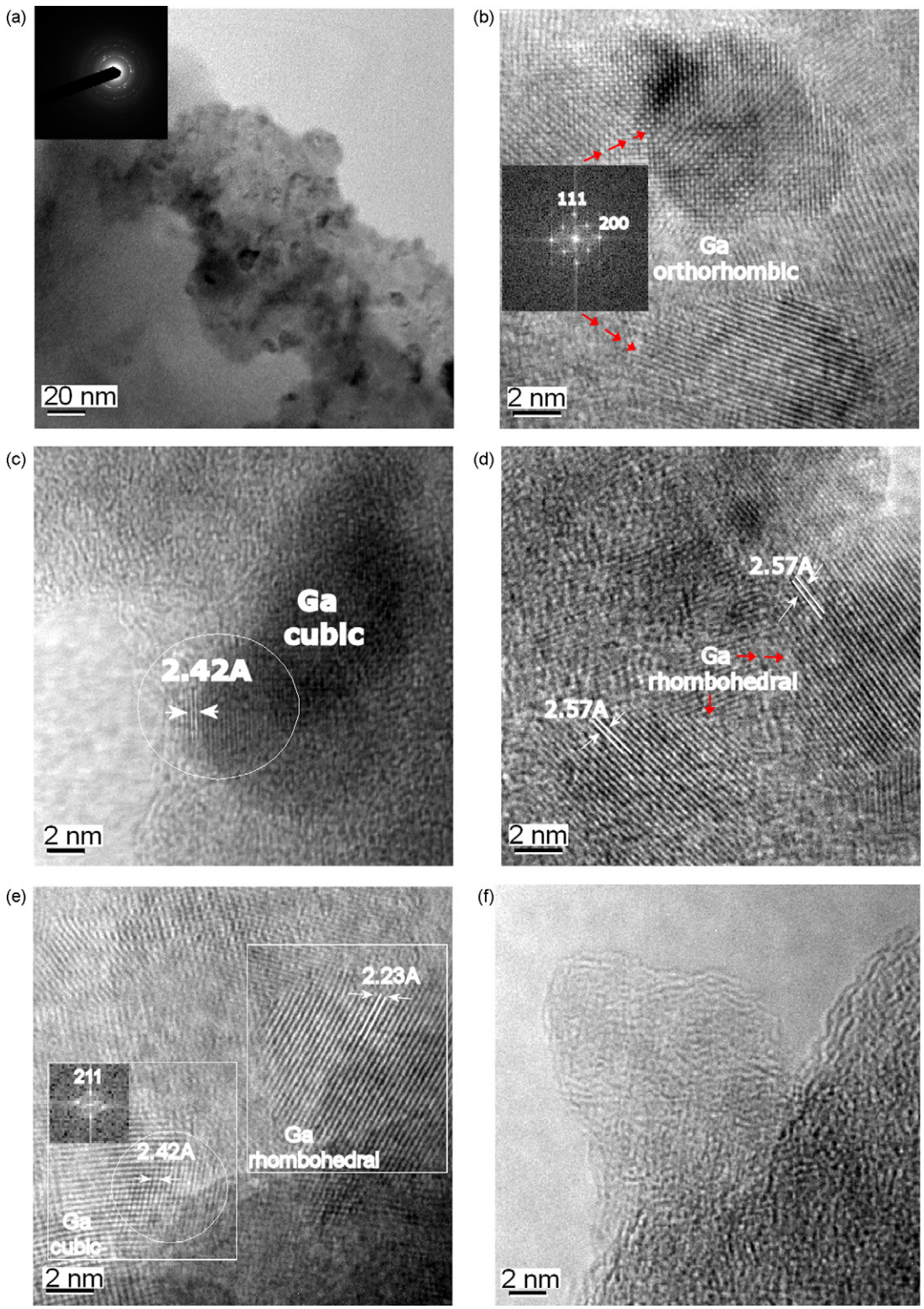

Fig. 7. Electron diffraction and HRTEM image of the film deposited from 10 Torr of ethyne (a) and HRTEM images of orthorhombic (b), cubic (c) and rhombohedral (d) nanograins, of a blend of rhombohedral and cubic nanograins (e) and of curved graphitic carbon (f).

The spectra of black films deposited from ethyne (Fig. 5) are dominated by G band at 1520-1540 cm^{-1} which shows asymmetry at lower wavenumbers belonging to a small contribution of D band. The spectrum of the film deposited on Ga has also a band at 2140 cm^{-1} assignable to stretching vibration of the C≡C bond.

The spectra of barely visible films deposited from n-hexane (Fig. 6) show more intense G and less intense D bands at 1580-1590 cm^{-1} and 1360 cm^{-1}, respectively. The films deposited on Cu substrate show, in addition, a band at 650 cm^{-1}, belonging to Cu surface. This band reveals that the carbonaceous films deposited from

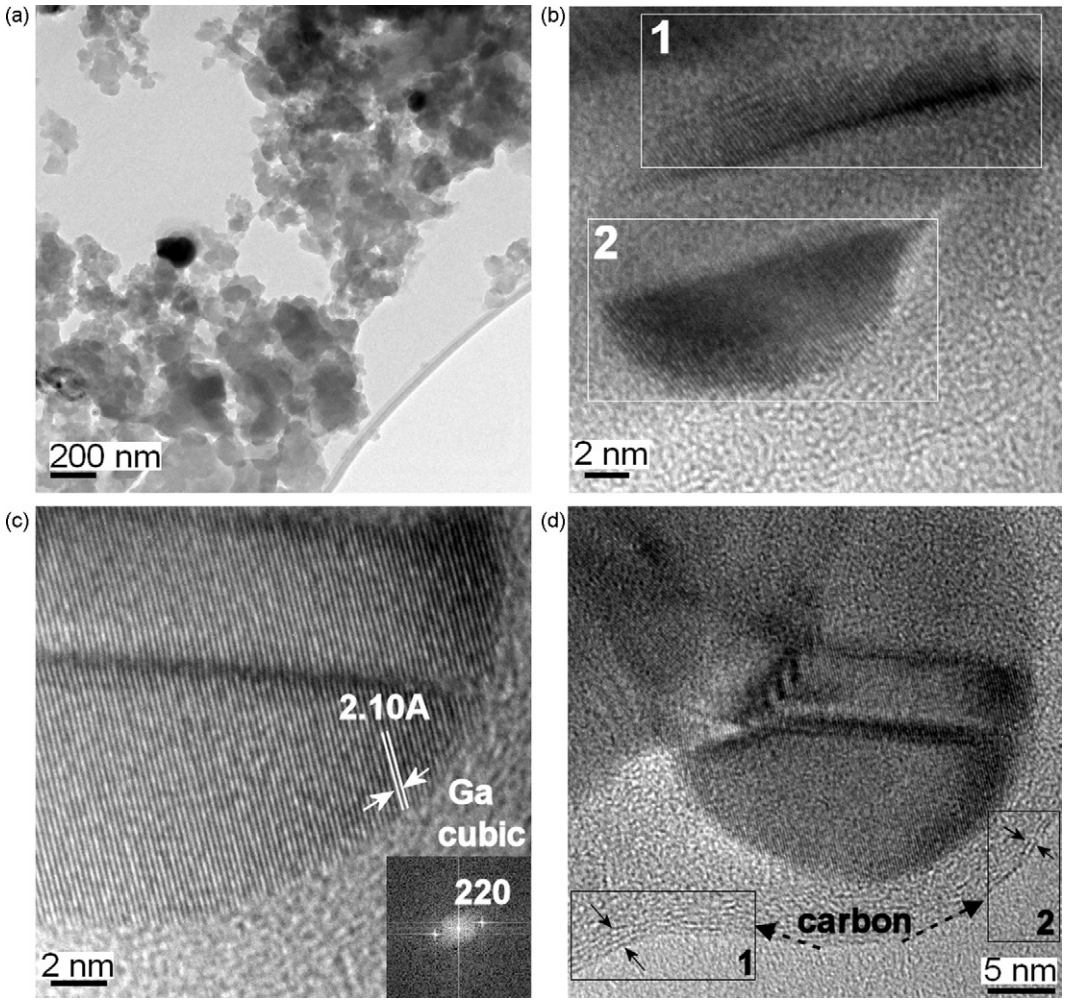

Fig. 8. HRTEM images of the film deposited from 10 Torr of benzene at low (a) and large (b-d) magnification) showing cubic Ga nanograins (designated as 1 and 2) separated by amorphous carbon (b), and cubic Ga nanograins covered with curved carbon environment (c,d).

n-hexane are much thinner than those deposited from benzene and ethyne.

It is known that (i) the positions of the G and D bands resemble those of graphitic a-C:H films and soot [21–23], (ii) the G peak position varies from 1520 cm^{-1} for amorphous carbons to 1590 cm^{-1} for glassy carbons [24] and higher values in this range correlate with low sp^3 content [25] and (iii) the G band reflects bond stretches of all pairs of sp^2 atoms in rings and chains and the D band relates to breathing modes of rings (e.g. [23,24,26]). Hence, we infer that the carbonaceous films from benzene and n-hexane resemble those of low sp^3 content glassy carbon and that the carbonaceous films from ethyne are similar to amorphous carbon, contain C≡C moieties and have less ring structures. We also deduce that the films deposited on Ga from benzene near the irradiated spot have more pronounced graphitic features due to more cyclic sp^2 structures.

The ATR FTIR spectra of the deposited films reveal that the films contain C-H bonds. Thus, the spectra of the films deposited on Cu substrate from benzene show weak absorption at 2840-3000 cm^{-1} and 3260-3330 cm^{-1}, respectively assignable to stretching vibrations of C(sp^3)-H and C(sp)-H bonds along with bands at 680 and 650 cm^{-1} corresponding to skeletal and deformation C-H vibrations. Similar spectral pattern, but not absorption at 3260-3330 cm^{-1}, is observed with films obtained from ethyne and hexane. None of these spectra show a ν(C=C) and a ν(C=O) band at 1600-1700 cm^{-1} that were observed in the carbonaceous films obtained from dielectric breakdown of hydrocarbons in the plasma plume of other metals (Ni, Co, Ag).

The X-ray diffraction of all films reveals no crystalline form of Ga or C and it shows only the fcc crystalline phase of the Cu substrate (syn-Cu). This finding indicates that the deposited films are principally composed of amorphous phase.

However, the HRTEM (high-resolution transmission electron microscopy) of the films show [27,28] crystalline nanoparticles of gallium. The orthorhombic, cubic and rhombohedral grains were identified in the film deposited from ethyne (Fig. 7), the cubic form was observed in the film deposited from benzene (Fig. 8), and cubic and tetragonal forms were disclosed in the deposit from hexane (Fig. 9). These Ga nanograins are immersed in carbonaceous phase and their identification is as follows. The lattice image of Ga with (111) and (200) planes (see FFT inset) corresponds (Fig. 7b) to orthorhombic Ga type cell with space group Abma (PDF ICDD 5-0601), the designated interlayer spacing d = 2.42 A (Figs. 7c and 7e) relates to (211) crystal planes in cubic Ga lattice (PDF 71-1834), and the lattice image of rhombohedral Ga is due to $d_{(205)}$=2.57 A and $d_{(125)}$ = 2.23 (PDF ICDD 71-0505) (Fig. 7,d and e). Strong spot arrays (see FFT inset in Fig. 8 c) were indexed on the basis of the cubic Ga type cell with space group I-43d and parameter a = 5.95A (PDF ICDD 71-1834). The SEAD pattern depicted in Fig. 9a corresponds to the rings indexed as (310) diffraction of cubic Ga and (101) diffraction of tetragonal Ga (PDF ICDD 71-1835). This pattern is in line with the HRTEM images confirming a

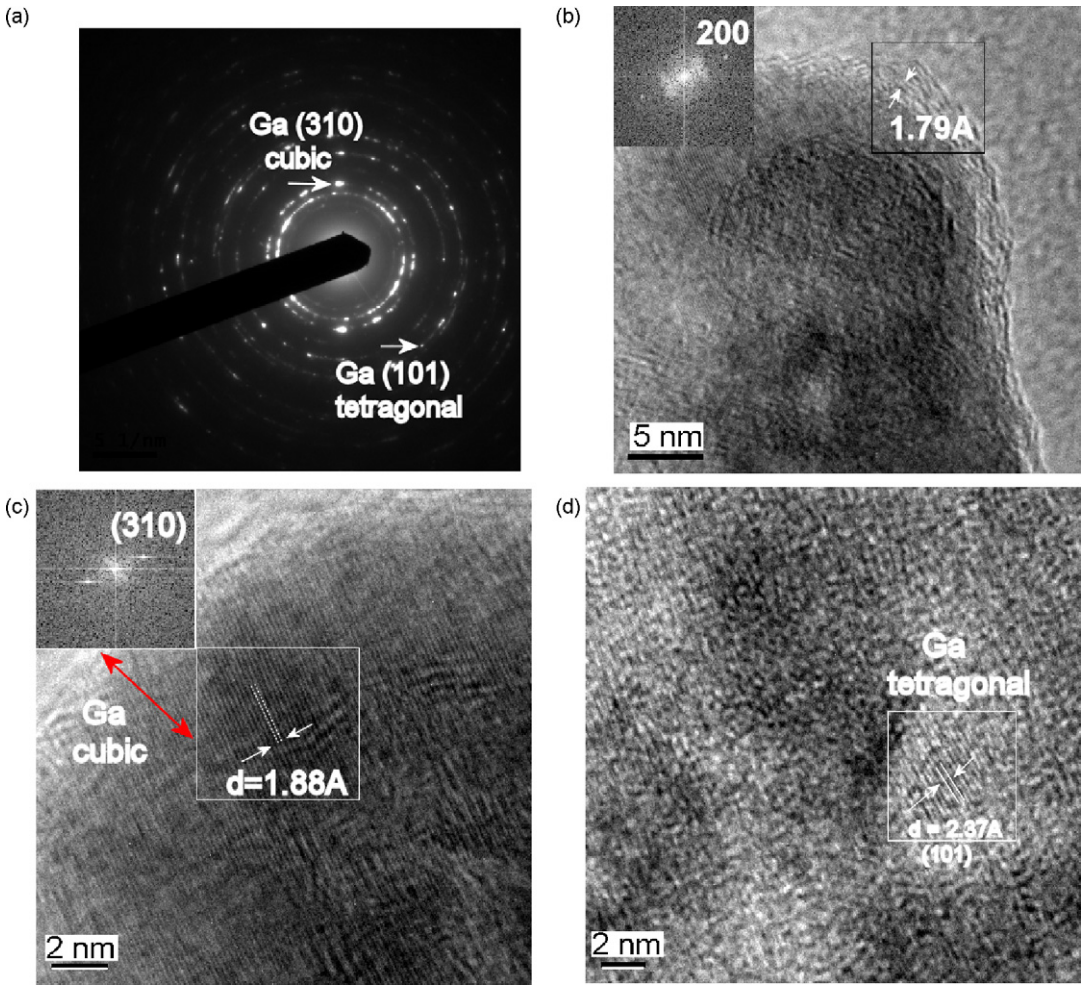

Fig. 9. HRTEM images of the film deposited from 10 Torr of n-hexane showing Ga nanoparticles enveloped with carbon shell (a,b) along with cubic (c) and tetragonal (d) nanograins.

co-existence of cubic (Fig. 9c) and tetragonal (Fig. 9d) Ga nanocrystals.

Gallium is known to have one stable (orthorhombic) phase at ambient pressure and two stable (face centered tetragonal and body centered cubic) phases at high pressure [28,29] along with several metastable phases at ambient pressure produced by supercooling the liquid or heating amorphous phase [30]. Our data thus show that the tetragonal, cubic and rhombohedral nanophases, normally not occurring at ambient pressure, can be formed at the specific IR laser irradiation conditions.

The HRTEM analysis indicates that carbon environment is a blend of amorphous phase containing Ga nanobjects embedded in a carbon shell (Figs. 7c,f; 8b,d and 9b) resembling curved arrangements of graphene layers [31,32] and considered as a primary stage of carbon graphitization [33]. This shell possesses interlayer spacing d = 1.79 A (Fig. 9b) belonging to (200) crystal planes of diamond-like structured carbon (PDF 43-1104, [34]) which is know to be produced at shock compression [34].

The complementary analyses of the deposited films thus reveal that the IR laser-deposited carbonaceous films can be described as nanocomposites having nanoobjects of amorphous and crystalline Ga immersed in a-C:H graphitic carbonaceous phase and enveloped by a shell of curved carbon that possesses both graphitic and diamond-like features.

We assume that the ambient-pressure unstable Ga forms are formed in a T jump during the laser pulse and can be stabilized by a fast (post-pulse) decrease in temperature and excess of simultaneously produced and deposited nanostructured carbon phase. The different nanocrystalline grains obtained in the different decomposing hydrocarbons (orthorhombic, cubic and rhombohedral obtained from ethyne, cubic obtained from benzene, and cubic and tetragonal obtained from hexane) are obviously less related to somewhat different temperatures in the laser plumes and are rather ascribed to differences in the post-pulse stabilization of hot metal clusters by different carbonizing species.

The reported ablative deposition of Ga/C films thus confirms suitability of the IR laser-induced process for fabrication of nano-sized metal particles isolated in carbonaceous phase and it shows that the process has a potential for synthesis of metastable nanostructures. The different nanocrystalline forms of Ga incorporated into depositing carbonaceous network obviously reflect different interaction between hot Ga nanoparticles and carbonizing species originating from benzene, ethyne or hexane.

4. Conclusions

The pulsed IR laser irradiation of Ga in 1 and 10 Torr of gaseous hydrocarbon (benzene, ethyne, n-hexane) results in ablation of Ga and adjacent dielectric breakdown-induced hydrocarbon decomposition. Both processes allow scattering of Ga nanobodies in the simultaneously gas-phase-produced carbonaceous phase and they result in the gas-phase deposition of Ga nanoparticles-containing carbonaceous films.

The volatile products of the hydrocarbon decomposition are characteristic for their pyrolyses which yield solid carbonaceous products having structure of a-C:H graphitic carbon. These solid products are more copious with benzene and ethyne than with hexane.

The Ga nanoparticles adopt different structures upon deposition and stabilization in the carbonaceous environment: the orthorhombic, cubic and rhombohedral grains were identified in the film deposited from ethyne, the cubic forms were observed in the film deposited from benzene and the cubic and tetragonal forms were found in the deposit from hexane.

We stress that only orthorhombic Ga exists at atmospheric pressure and that the other forms occur only at high pressures. The reported ablative deposition of Ga thus allows alternative approach to the formation of ambient-pressure unstable Ga phases.

Acknowledgements

The authors thank the Czech Science Foundation (GAAVCR grant no. 400720619) and the Ministry of Education. Youth and Sports of the Czech Republic (grant no. LC523) for funding this research. Thanks are due to Dr. Bezdička for the XRD analysis.

References

[1] K.-Q. Ma, J. Liu, Nano liquid-metal fluid as ultimate coolant, Phys. Lett. A 361 (2007) 252–256.
[2] Y. Gao, Y. Bando, Carbon nanothermometer containing gallium, Nature 415 (2002) 599.
[3] K.F. MacDonald, A.V. Krasavin, N.I. Zheludev, Ga-Al and Ga-Ag nano-structured films for active plasmonics applications., Pacific Rim Conference on Lasers and Electro-Optics, Tokyo (2005) 877–878.
[4] K.F. MacDonald, A.V. Krasavin, N.I. Zheludev, Gallium/aluminium nanocomposite for nonlinear-optical and plasmonic switching applications. Quantum Electronics and Laser Science Conference, Long Beach, CA, (2006) QMF4.
[5] M.K. Sunkara, S. Sharma, R. Miranda, G. Lian, E.C. Dickey, Bulk synthesis of silicon nanowires using a low-temperature vapor-liquid-solid method, Appl. Phys. Lett. 79 (2001) 1546–1548.
[6] Z.W. Pan, S. Dai, D.B. Beach, N.D. Evans, D.H. Lowndes, Gallium-mediated growth of multiwall carbon nanotubes, Appl. Phys. Lett. 82 (2003) 1947–1949.
[7] Z.W. Pan, Z.R. Dai, C. Ma, Z.L. Wang, Molten gallium as a catalyst for the large-scale growth of highly aligned silica nanowires, J. Am. Chem. Soc. 124 (2002) 1817–1822.
[8] P.C. Wu, C.G. Khoury, T.-H. Kim, Y. Yang, M. Losurdo, G.V. Bianco, T. Von-Dinh, A.S. Brown, H.O. Everitt, Demonstration of Surface-enhanced Raman scattering by tunable, plasmonic gallium nanoparticles, J. Am. Chem. Soc. 131 (2009) 12032–12033.
[9] P.C. Wu, T.-H. Kim, A.S. Brown, M. Losurdo, G. Bruno, H.O. Everitt, Real-time plasmon resonance tuning of liquid Ga nanoparticles by *in situ* spectroscopic ellipsometry, Appl. Phys. Lett. 90 (2007), 103119 (3 pages).
[10] P.C. Wu, M. Losurdo, T.-H. Kim, S. Choi, G. Bruno, A.S. Brown, In situ spectroscopic ellipsometry to monitor surface plasmon resonant group-III metals deposited by molecular epitaxy, J. Vac. Sci. Technol. B 25 (2007) 1019–1023.
[11] J. Zhan, Y. Bando, J. Hu, D. Golberg, H. Nakanishi, Liquid gallium columns sheathed with carbon: bulk synthesis and manipulation, J. Phys. Chem. B 109 (2005) 11580–11584.
[12] B. Fazio, O. Maragò, E. Arimondo, C. Spinella, C. Bongiorno, G. D'Arrigo, Towards fabrication of ordered gallium nanostructures by laser manipulation of neutral atoms:study of self-assembling phenomena, Superlatt. Microstruct. 36 (2004) 219–226.
[13] M. Santos, L. Díaz, J. Camacho, M. Urbanová, D. Pokorná, J. Šubrt, S. Bakardjieva, Z. Bastl, J. Pola, IR Laser-induced Metal Ablation and Dielectric Breakdown in Benzene, Infrared Phys. Technol. 53 (2010) 23–28.
[14] J. Pola, M. Urbanová, D. Pokorná, J. Šubrt, S. Bakardjieva, P. Bezdička, Z. Bastl, IR Laser-induced Formation of Amorphous Co-C Films with Crystalline Co, Co_2C and Co_3C Nanograins in a Graphitic Shell, J. Photochem. Photobiol. A 210 (2010) 153–161.
[15] M. Urbanová, D. Pokorná, S. Bakardjieva, J. Šubrt, Z. Bastl, P. Bezdička, J. Pola, IR Laser-induced Ablation of Ag in Dielectric Breakdown of Gaseous Hydrocarbons: Co-existence of Metastable hcp and Stable fcc Ag Nanostructures in C:H Shell. J. Photochem. Photobiol., A, doi:10.1016/j.jphotochem.2010.05.009.
[16] J.H. Kiefer, L.J. Mizerka, M.R. Patel, H.-C. Wei, A shock tube investigation of major pathways in the high temperature pyrolysis of benzene, J. Phys. Chem. 89 (1985) 2013–2019.
[17] M.H. Back, Mechanism of the pyrolysis of acetylene, Can. J. Chem. 49 (1971) 2199–2204.
[18] H. Ogura, Pyrolysis of acetylene behind shock waves, Bull. Chem. Soc. Jap. 50 (1977) 1044–1050.
[19] K.H. Ebert, H.J. Ederer, G. Isbarn, The thermal decomposition of n-hexane, Int. J. Chem. Kinet. 15 (1983) 475–502.
[20] P. Zámostný, Z. Bělohlav, L. Starkbaumová, J. Patera, Experimental study of hydrocarbon structure effects on the composition of its pyrolysis products, J. Anal. Appl. Pyrol. 87 (2010) 207–216.
[21] J. Schwan, S. Ulrich, K. Jung, H. Ehrhardt, R. Samlenski, R. Brenn, Deposition of ta-C:H films by r.f. plasma discharges, Diamond Relat. Mater. 4 (1995) 304–308.
[22] A.C. Ferrari, J. Robertson, Interpretation of Raman spectra of disordered and amorphous carbon, Phys. Rev. B 61 (2000) 14095–14107.
[23] P.K. Bachmann, D.U. Wiechert in Diamond and Diamond-Like Films and Coatings, Eds. R.E. Clausing et al., Pergamon Press, 1991, p. 677.
[24] M. Yoshikawa, G. Katagiri, A. Ishida, A. Ishitani, Raman spectra of diamondlike amorphous carbon films., Solid State Commun. 66 (1988) 1177–1180.
[25] S. Prawer, K.W. Nugent, Y. Lifshitz, G.D. Lempert, E. Grossman, J. Kulik, I. Avigal, R. Kalish, Systematic variation of the Raman spectra of DLC films as a function of sp^2:sp^3 composition, Diamond Relat. Mater. 5 (1996) 433–438.
[26] R.O. Dillon, J.A. Woollam, V. Katkanant, Use of Raman scattering to investigate disorder and crystalline formation in as-deposited and annealed carbon films, Phys. Rev. B 29 (1984) 3482–3489.
[27] JCPDS PDF-2 database, release 54, International Centre for Diffraction Data, Newton Square PA, U.S.A., 2004.
[28] L. Bosio, Crystal structures of Ga(II) and Ga (III), J. Chem. Phys. 68 (1978) 1221–1223.
[29] L. Bosio, A. Defrain, I. Epelboin, Sur le polymorphisme du gallium a haute pression, J. Chim. Phys. 75 (1978) 145–146.
[30] Z. Liu, Y. Bando, M. Mitome, J. Zhan, Unusual freezing and melting of gallium encapsulated in carbon nanotubes, Phys. Rev. Lett. 93 (2004), 095504, 4 pages and refs. therein.
[31] I Morjan, I. Voicu, F. Dumitrache, I. Sandu, I. Soare, R. Alexandrescu, E. Vasile, I. Pasuk, R.M.D. Brydson, H. Daniels, B. Rand, Carbon nanopowders from continuous-wave CO_2 laser-induced pyrolysis of ethylene, Carbon 41 (2003) 2913–2921.
[32] N. Herlin, I. Bohn, C. Reynaud, M. Cauchetier, A. Galvez, J.N. Rouzaud, Nanoparticles produced by laser pyrolysis of hydrocarbons: analogy with carbon cosmic dust, Astron. Astrophys. 330 (1998) 1127–1135.
[33] I. Morjan, I. Voicu, R. Alexandrescu, I. Pasuk, I. Sandu, F. Dumitrache, I. Soare, T.C. Fleaca, M. Ploscaeu, V. Ciupina, H. Daniels, A. Westwood, B. Rand, Gas composition in laser pyrolysis of hydrocarbon-based mixtures: Influence on soot morphology, Carbon 42 (2004) 1269–1273.
[34] H. Hirai, K. Kondo, A new crystalline form of carbon under shock compression, Proc. Jpn. Acad. B 67 (1991) 22–26.